Comparison of Wild-Type and nifV Mutant Molybdenum-Iron Proteins of Nitrogenase from *Klebsiella pneumoniae* by ENDOR Spectroscopy

Anne E. True,[†] Paul McLean,[‡,§] Mark J. Nelson,[‡,∥] W. H. Orme-Johnson,[‡] and Brian M. Hoffman*,[†]

Contribution from the Department of Chemistry, Northwestern University, Evanston, Illinois 60208, and the Department of Chemistry, Massachusetts Institute of Technology, Cambridge, Massachusetts 02139. *Received October 20, 1988*

Abstract: Electron nuclear double resonance (ENDOR) studies of native and isotopically enriched MoFe proteins allow individual characterization of the atoms in the catalytically active FeMo-cofactor (FeMo-co) cluster of the nitrogenase MoFe protein. This paper presents ^{1}H, ^{57}Fe, ^{95}Mo, and ^{14}N ENDOR measurements in a comparison of the MoFe protein isolated from wild-type *Klebsiella pneumoniae* (Kpl WT) and the nifV mutant of this organism (NifV$^-$ Kpl), which contains an altered form of the FeMo-co cluster. Single-crystal-like ^{57}Fe ENDOR measurements show that one of the five iron sites in NifV$^-$ Kpl has magnetic properties different from those of the wild-type protein. Proton ENDOR studies reveal an additional set of exchangeable protons that is present in NifV$^-$ Kpl but not Kpl WT. ^{95}Mo ENDOR measurements show that the molybdenum site is perturbed in the cofactor. These differences are the first to be detected by physical methods and may be due to the replacement, addition, or subtraction of a non-sulfur ligand weakly bound at or near the molybdenum atom; the possible identity of such a ligand is discussed. Evidence also is presented for nitrogen coupled to the FeMo-co cluster in both proteins.

The molybdenum-iron protein of nitrogenase contains 2 mol of molybdenum, approximately 30 mol of iron, and approximately 30 mol of acid-labile sulfur/mol of peptide component. These metals are grouped into six metal clusters: four P clusters and two molybdenum-iron cofactors.[1-6] Accurate chemical and spectroscopic assignment of these molybdenum, iron, and sulfur atoms into individual clusters and the investigation of the structure of those clusters constitutes much of the recent progress in the study of nitrogenase. In particular, the molybdenum-iron cofactor has been extensively studied because there is evidence that these clusters are the active site of the protein.[6]

The nifV mutant of *Klebsiella pneumoniae* produces mutant MoFe protein (NifV$^-$ Kpl) that will reduce C_2H_2 but not N_2 in vivo.[7,8] The phenotype of the nifV mutant is transferred to wild-type (WT) apoprotein upon addition of mutant cofactor,[7] and thus the composition or structure of the mutant cofactor differs from that of the wild type. Chemical analysis has shown the metal composition of WT and NifV$^-$ (V$^-$) cofactor to be identical,[8] and EXAFS spectroscopic measurements[9,10] have failed to detect a difference in the S and Fe environments of molybdenum. Electron nuclear double resonance (ENDOR) measurements provided the first observation of an effect of the mutation on the physical properties of the cofactor, a difference in the characteristics of molybdenum.[10] V$^-$ mutants apparently lack the ability to synthesize homocitrate, which is reported to restore in vitro synthesis of cofactor by extracts of nifV$^-$ strains.[8c] One possibility is that homocitrate is required as a coordinating reactant during the synthesis of cofactor. Homocitrate or a derivative thereof may end up in finished cofactor but this point has not been settled.

Because the nature of the ligands in molybdenum complexes greatly influences their ability to bind N_2, the presence of the V gene product might modify the ligation of metals by the addition or deletion of ligands or reorientation of existing bonds.[7a] The present paper extends the use of ENDOR spectroscopy of ^{57}Fe-, ^{95}Mo-, and ^{100}Mo-enriched samples[10,11] of WT and V$^-$ Kpl to probe the nature of the alteration in the molybdenum-iron cofactor.

Materials and Methods

Isotopically enriched samples of wild-type and NifV$^-$ Kpl were prepared in Tris-HCl or TES-HCl buffer solutions as described.[11] The ENDOR spectrometer is based on a Varian Associates E-109 EPR spectrometer as described elsewhere.[11] The ENDOR signals were observed as an intensity change in the 100-kHz field-modulated, dispersion-mode EPR signal and accumulated in the computer. Each ENDOR resonance was the subject of at least four independent measurements. The proton and iron resonances reported here have narrow line widths[11c] and were acquired with exceptionally good signal-to-noise. Because of this and the high accuracy of the frequency synthesizer, resonance frequencies could be measured with exceptional accuracy; in particular for ^{57}Fe, the uncertainties are ±0.03 MHz in most cases.

Table I g Values[a] and Zero-Field Splitting Parameters of Various Samples of the Wild-Type and Nif V Mutant Kpl

	$S' = {}^1/_2$[b]		$S = {}^3/_2$		
sample	g_1'	g_2'	g	$\lambda = E/D$	Δ,[c] cm^{-1}
Kpl	4.330	3.658	2.001	0.056	12.5
NifV$^-$ Kpl	4.334	3.664	2.004	0.056	12.6

[a] The average electronic parameters when several samples were employed. Errors are ±0.004. [b] In all cases $g_3' = g = 2.01$. [c] Errors in this measurement are ±0.5 cm^{-1}.

[†] Northwestern University.
[‡] Massachusetts Institute of Technology.
[§] Current address: Biotechnica Int. Inc., Cambridge, MA 02139.
[∥] Current address: E. I. Du Pont de Nemours, Inc. Wilmington, DE 19898.

(1) Nelson, M. J.; Lindahl, P. A.; Orme-Johnson, W. H. In *Advances in Inorganic Biochemistry*; Eichorn, G. L., Marzilli, L. G., Eds.; Elsevier: New York, 1981; pp 1-40.
(2) Mortenson, L. E.; Thorneley, R. N. F. *Annu. Rev. Biochem.* **1979**, *48*, 387-418.
(3) Brill, W. J. *Microbiol. Rev.* **1980**, *44*, 449-467.
(4) Yates, M. G. In *Biochemistry of Plants*; Miflin B. J., Ed.; Academic Press: New York, 1980; pp 1-64.
(5) Robson, R. L.; Postgate, J. R. *Annu. Rev. Microbiol.* **1980**, *34*, 183-207.
(6) Orme-Johnson, W. H. *Annu. Rev. Biophys. Chem.* **1985**, *14*, 419-459.
(7) (a) McLean, P. A. Ph.D. Thesis, University of Sussex, UK, 1981. (b) McLean, P. A.; Dixon, R. A. *Nature (London)* **1981**, *292*, 655-656. (c) McLean, P. A.; Smith, B. E.; Dixon, R. A. *Biochem. J.* **1983**, *211*, 589-597.
(8) (a) Hawkes, T. R.; McLean, P. A.; Smith, B. E. *Biochem. J.* **1984**, *217*, 317-321. (b) Hawkes, T. R.; Lowe, D. J.; Smith, B. E. *Biochem. J.* **1983**, *211*, 495-497. (c) Hoover, T. R.; Robertson, P. D.; Cerny, R. L.; Hayes, R. N.; Imperial, J.; Shah, V. K.; Ludden, P. W. *Nature* **1987**, *329*, 855-857.
(9) Eidsness, M. K.; Flank, A. M.; Smith, B. E.; Flood, A. C.; Garner, C. D.; Cramer, S. P. *J. Am. Chem. Soc.* **1986**, *108*, 2746-2747.
(10) McLean, P. A.; True, A. E.; Nelson, M. J.; Chapman, S.; Godfrey, M. R.; Teo, B.-K.; Orme-Johnson, W. H.; Hoffman, B. M. *J. Am. Chem. Soc.* **1987**, *109*, 943-945.
(11) (a) Venters, R. A.; Nelson, M. J.; McLean, P. A.; True, A. E.; Levy, M. A.; Hoffman, B. M.; Orme-Johnson, W. H. *J. Am. Chem. Soc.* **1986**, *108*, 3487-3498. (b) True A. E.; Nelson, M. J.; Venters, R. A.; Orme-Johnson, W. H.; Hoffman, B. M. *J. Am. Chem. Soc.* **1988**, *110*, 1935-1943. (c) True, A. E. Ph.D. Dissertation, Northwestern University, 1988.

0002-7863/90/1512-651$02.50/0

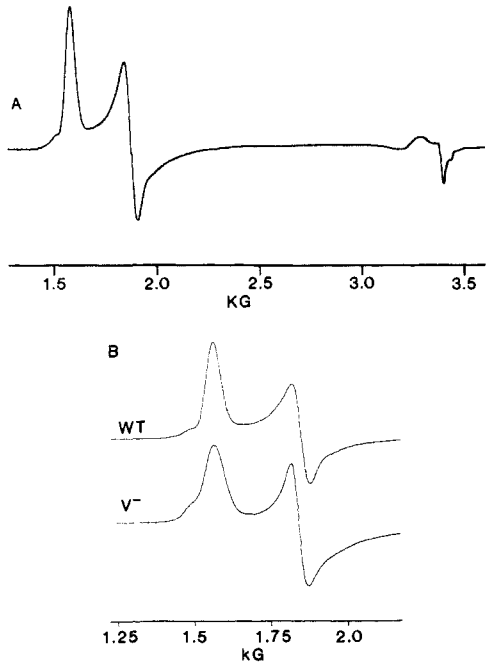

Figure 1. Absorption-derivative EPR spectra of the ^{57}Fe-enriched wild-type and NifV$^-$ mutant MoFe proteins of nitrogenase from *K. pneumoniae*. EPR spectra of (A) the wild-type and (B) the g_1-g_2 region of the wild-type and nifV mutant of the *K. pneumoniae* MoFe protein of nitrogenase. Conditions: microwave power, 0.20 mW; microwave frequency, 9.52 GHz; 100-kHz field modulation, 4 G; T = 2 K.

Results and Discussion

Resting State Enzyme. EPR Results. The absorption EPR spectra for the wild-type Kp1 and the nifV Kp1 mutant of *K. pneumoniae*, as shown in Figure 1, are characteristic of the lower Kramers' doublet ($m_S = \pm^1/_2$) of a metal center with a total electron spin of $S = {}^3/_2$.[11] The spin quartet of this system is split into two Kramers' doublets separated by the zero-field splitting energy Δ, where Δ is defined by[12]

$$\Delta = 2D(1 + 3\lambda)^{1/2} \tag{1}$$

and the rhombicity is measured by $\lambda = E/D$, where D and E are the axial and rhombic zero-field splitting parameters. When this spectrum is treated in terms of an effective spin, $S' = {}^1/_2$, its g' values can be used to obtain the ratio of the zero-field parameters characterizing the rhombicity of the zero-field splitting tensor (λ), along with a value of $g_\perp$ in the $S = {}^3/_2$ representation, through inversion of eq 2a.[13]

$$g'_{2(-),1(+)} = g_\perp\left[1 + \frac{1 \mp 3\lambda}{(1 + 3\lambda)^{1/2}}\right] \tag{2a}$$

$$g_3' = g_\parallel \tag{2b}$$

The EPR line width for the g_1' feature of the mutant protein (~50 G) is consistently broader than that of the wild-type protein (~40 G). The g_1' feature of both proteins contains a pronounced shoulder, but its relative intensity is larger in the mutant protein, suggesting that the signal from NifV$^-$ Kp1 contains a larger contribution from a second minority component. The major component of both the wild-type and mutant Kp1 spectra has g' values that are the same within ±0.01.[7c] Table I contains the

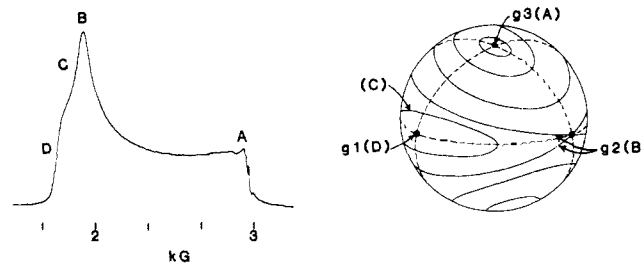

Figure 2. Rapid-passage dispersion EPR spectrum of the ^{57}Fe-enriched wild-type MoFe protein and unit sphere with axes representing the **g** tensor; curves on the surface are of constant g. Positions at the extreme edges of the EPR spectrum near either g_3' (position A) or g_1' (position D) give single-crystal-like ENDOR patterns. Positions at intermediate fields (such as C and B) involve a well-defined range of molecular orientations, as indicated on the sphere. Conditions are as described in Figure 1.

experimental g' values as well as $g_\perp$ and λ.

ENDOR Analysis. For a single-crystal ENDOR measurement from a nucleus with spin I, in first order one expects $4I$ ENDOR transitions having as approximate values for the transition frequencies[12]

$$\nu_{\pm(m_i)} = \left|\pm\frac{A^{N\prime}}{2} + \nu_N + 3P^N(2m_I - 1)/2\right| \tag{3}$$

where $-I + 1 \le m_I \le I$, $A^{N\prime}$ is the angle-dependent hyperfine coupling constant in the $S' = {}^1/_2$ representation and P^N is the angle-dependent quadrupole splitting. When the lower Kramers' doublet is treated as an $S' = {}^1/_2$ system and the electronic Zeeman and hyperfine tensors are coaxial, the principle axis values of the hyperfine interaction tensor, A_j', are related to the principal axis values of the hyperfine Hamiltonian in the $S = {}^3/_2$ representation, by[12]

$$A_j' = A_j g_j'/g_j \tag{4}$$

where A_j', g_j', and g_j are the hyperfine coupling constants and electronic g values in the $S' = {}^1/_2$ and $S = {}^3/_2$ systems, respectively; a more general relation is presented below.

The quadrupole splitting Hamiltonian for a nucleus of spin I is expressed in terms of a traceless tensor, $P_1^N + P_2^N + P_3^N = 0$, where $P_i^N = e^2q_iQ/[2hI(2I - 1)]$; the angle-dependent quadrupole splitting constant of eq 3, P^N, is specified so that $P_i^N = P^N$ for a principal axis direction. Alternatively, the quadrupole interaction can be formulated in terms of the component of largest magnitude, P_3^N, and the asymmetry parameter, $0 \le \eta = (P_1^N - P_2^N)/P_3^N \le 1$. The goals of this paper are adequately served by eq 3 and 4.

The Larmor frequency for an isolated nucleus within the ground-state EPR-active $m_S = \pm^1/_2$ doublet is given by $\nu_N^0 = g_N\beta_nB_0$ where g_N is the intrinsic g factor. However, the $m_S = \pm^3/_2$ electronic spin doublet that arises from the zero-field splitting of the total spin $S = {}^3/_2$ ground state of the MoFe protein provides a low-lying electronic state that gives rise to a large anisotropic pseudo-nuclear Zeeman effect in the $m_S = \pm^1/_2$ doublet.[12] This leads to an effective nuclear Larmor frequency as given by $\nu_N = g^N\beta_nB_0$, where g^N is an angle-dependent splitting factor determined by the effective nuclear $\mathbf{g}^N$ tensor that is coaxial with the zero-field splitting tensor and has principal components[11]

$$g_3^N = g_n$$

$$g_j^N = g_N\{1 + {}^3/_2(g\beta/g_N\beta_n)(A_j/\Delta)\}_{j=1,2} \tag{5}$$

Equation 5 ignores the rhombic splitting of the electron **g** tensor, which causes further rhombic splitting of the nuclear $\mathbf{g}^{(N)}$ tensor; the general equation has been derived and the correction has been found to be unimportant for $\lambda \ll 1$.[11] In particular, the direction of $\mathbf{g}^N$ corresponds to that of the axial zero-field splitting component (D) and thus to the g_3 axis of the electron Zeeman $\mathbf{g}'$ tensor. For nuclei with small g_N, such as ^{57}Fe and ^{95,97}Mo, the effect can be large, and depending on the magnitude of A_j^N/Δ and the sign of

(12) (a) Abragam, A.; Bleaney, B. In *Electron Paramagnetic Resonance of Transition Ions*; Clarendon Press: Oxford, UK, 1970. (b) Atherton, N. M. In *Electron Spin Resonance*; Halstead: New York, 1973. (c) Carrington, A.; McLaughlin, A. D. In *Introduction to Magnetic Resonance*; Harper and Row: New York, 1967.

(13) Hoffman, B. M.; Weschler, C. J.; Basolo, F. *J. Am. Chem. Soc.* **1976**, *98*, 5473-5482.

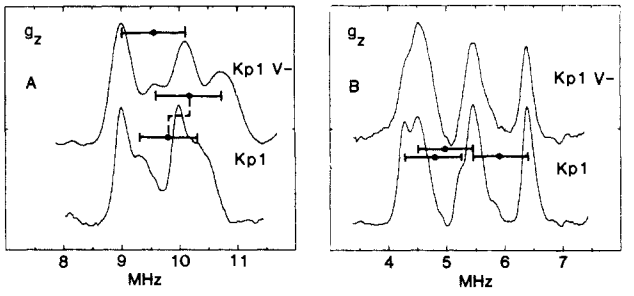

Figure 3. ^{57}Fe ENDOR spectra at g_3 of (A) the two higher frequency (a^1, a^2) and (B) the three lower frequency (b^1, b^2, b^3) iron sites of Kp1 WT and NifV$^-$ Kp1. The intensities of spectra for the two proteins were normalized. The assignments of the five Larmor-split doublets are indicated (|—|), as are the frequencies corresponding to $A/2$ (●). Conditions: H_0 = 3362 G; T = 2 K; microwave power, 0.63 mW; microwave frequency, 9.52 GHz; 100-kHz field modulation, 4 G; rf power 30 W; rf scan rate, 3.0 MHz/s. Each spectrum represents ca. 3000 scans.

A_j^N, ν_N may range from $\nu_N \gg \nu_N^0$ through $\nu_N \sim 0$ and even $\nu_N < 0$, the latter corresponding merely to a reversal of the line positions.

The MoFe protein samples employed in this study are frozen solutions and thus contain magnetic centers of random orientations. However field positions at the high-field edge, g_3' (position A, Figure 2), and the extreme low-field edge, below g_1' (position D, Figure 2), will yield single-crystal-like ENDOR patterns associated with those molecules having a magnetic field directed along the corresponding g' axes. ENDOR signals at an intermediate magnetic field, g', will arise from a well-defined subset of orientations for which the angle-dependent g values equals g'. ENDOR obtained at fields away from the EPR spectrum edges are amenable to analysis through our theory of polycrystalline spectra.[11b,14,15]

^{57}Fe ENDOR Results. For ^{57}Fe, $I = {}^1/_2$ and the quadrupole term in eq 3 vanishes. With the field set to give a single-crystal-like ENDOR spectrum at g_1', each iron site is expected to give a Larmor doublet centered at $A_1'/2$ and split by twice the effective nuclear Zeeman interaction. When the magnetic field is set to the extreme high-field edge of the EPR spectrum of Kp1 the ENDOR pattern exhibits five such doublets (Figure 3). These peaks are not present in the ^{56}Fe samples and represent ^{57}Fe resonances from five distinct types of iron nuclei within the FeMo-co cluster of the Kp1 protein.[11] The hyperfine couplings of the ^{57}Fe nuclei consists of two groups: one is centered at an average coupling of $A/2$ at ~5.5 MHz and the other at ~9.5 MHz. Figure 3 compares the ^{57}Fe pattern at g_3 of wild-type Kp1 and NifV$^-$ Kp1. In the NifV$^-$ Kp1 spectra, the highest frequency doublet has shifted to higher frequency by 0.2 MHz, or ~2%. The lowest frequency doublet of the mutant also appears to have shifted slightly to higher frequency, but this apparent change may be due to a loss of resolution rather than any change in the hyperfine coupling constant. The other ^{57}Fe nuclei have the same hyperfine coupling as the wild-type protein (Table II).

^{57}Fe ENDOR spectra were also taken with the magnetic field at the low-field edge of the EPR spectrum, both at the g_1' peak and at the low-field half-height feature of the g_1' peak in the absorption derivative EPR spectrum. Use of a field lower than g_1' ensures that the resonances are only from the molecules with their magnetic field directed along the g_1' axis.[14,15] The coupling constants derived from measurements at g_1' differ slightly from the limiting values obtained at lower fields, but the signal is weaker and possible contributions from the minority component visible in the EPR spectrum are enhanced. Comparisons at g_1' of wild-type and NifV$^-$ Kp1 gave results analogous to comparisons of the two proteins at a lower field, and for convenience, the results given in this study were obtained at g_1'. It should be noted that extreme care must be taken to obtain data at similar features on the EPR spectra for comparing measurements from different proteins because of changes in their respective g_j values (eq 4).

In principle, at these low fields in both the wild-type and NifV$^-$ proteins, there might be contributions to the ENDOR spectra from the minority components, which make a larger relative contribution to the EPR spectrum at g' values larger than g_1' (see Figure 1). However, the spectra taken at lower magnetic fields show no significant difference from spectra obtained at g_1' and the hyperfine coupling values change in a smooth continuous manner as g' is increased from g_1', as expected for spectra from a single species. Either the ENDOR resonances obtained at these low fields are attributable only to the major component of the EPR spectra or else the minority and majority components give ENDOR patterns that are indistinguishable.

Both wild-type and NifV$^-$ Kp1 exhibit six ^{57}Fe ENDOR peaks with the field set near g_1' (Figure 4). As previously reported,[11] peaks 1–4 can be assigned to two iron sites, B^1 and B^2, with small positive hyperfine couplings. For the wild-type protein the average frequency of peaks 1 and 2, after correction to the $S = {}^3/_2$ representation by eq 4, leads to a hyperfine coupling constant for site B^2 of $A_1(B^2)$ = +8.75 (3) MHz, while peaks 3 and 4 yield a hyperfine coupling for site B^1 of $A_1(B^1)$ = 11.18 (3) MHz. The Larmor splitting of peaks 1 and 2 from site B^2 (0.74 MHz) and of peaks 3 and 4 from site B^1 (0.83 MHz) is reproduced upon consideration of the pseudo-nuclear Zeeman effect (eq 5) by using Δ(WT) = 12.5 (±0.5) cm^{-1}.

As previously described,[11] peaks 5 and 6 can be assigned to two iron sites with negative hyperfine coupling. In such a case the direct and pseudo-nuclear Zeeman effects are opposed, and as expressed in eq 5 with Δ = 12.5 cm^{-1} for the sites in question, they roughly cancel and $2\nu_{Fe}$ becomes unresolvably small.[11] In addition, the high-frequency shoulder at 13.5 MHz on peak 4 of the B^1 site represents the single peak of an additional site, A^3, having a negative coupling and no resolved Larmor splitting (Table II); this peak splits out and is clearly seen at other fields.[11b]

At g_1' the B^2 site in NifV$^-$ Kp1 has a hyperfine coupling constant in the $S = {}^3/_2$ representation that is shifted to higher frequency by ~2% [$A_1(B^2)$ = 8.91 (3) MHz] relative to that for the wild-type Kp1 protein. In contrast, although peak A^1 appears somewhat broadened and there are perhaps some changes in resolution of peaks 3 and 4, the other ^{57}Fe ENDOR frequencies at g_1' are unchanged within the experimental uncertainty of ±0.03 MHz (Figure 4; Table II). The Larmor splittings of sites B^1 and B^2 of the mutant protein are the same as the wild-type protein and thus the value of Δ is unchanged by the nifV mutation. Comparisons of site A^3 at a higher field, g' = 4.14, where the ν_+ of site B^1 peak no longer coincides with the A^3 resonance, confirm that the pattern of site A^3 also is not measurably altered in the NifV$^-$ protein.

It seems reasonable to correlate the iron site that gives the B^2 signal at g_1' with the highest frequency iron doublet at g_3', since these are the only peaks that differ in the mutant protein. However, there is no direct evidence for this correspondence. Thus, of the five sites distinguished in the ^{57}Fe ENDOR spectra of Kp1

Table II. ^{57}Fe Hyperfine Coupling Constants (MHz) in the $S = {}^3/_2$ Representation for the Kp1 and NifV$^-$ Kp1 Proteins[a]

	site				
at g_1'	A^1	A^2	A^3	B^1	B^2
Kp1	−20.58	−14.49	~12	11.18	8.75
NifV$^-$ Kp1	−20.63	−14.50	~12	11.19	8.91
at g_3'	a^1	a^2	b^1	b^2	b^3
Kp1[b]	18.80	19.42	9.38	9.80	11.65
NifV$^-$ Kp1	18.87	19.85	9.45	9.83	11.68

[a] All errors are ±0.02 MHz; correlations have not been made between resonances at g_1' and g_3'. [b] These values differ from those reported in ref 11a by more than the errors stated in footnote a. The present values are correct. The earlier experiments agree with those reported here, but the older tabulated values were subjected to an erroneous correction factor in the conversion from $S' = {}^1/_2$ to $S = {}^3/_2$ representations.

(14) Hoffman, B. M.; Martinsen, J.; Venters, R. A. *J. Magn. Reson.* **1984**, *59*, 110–123.
(15) Hoffman, B. M.; Martinsen, J.; Venters, R. A. *J. Magn. Reson.* **1985**, *62*, 537–542.

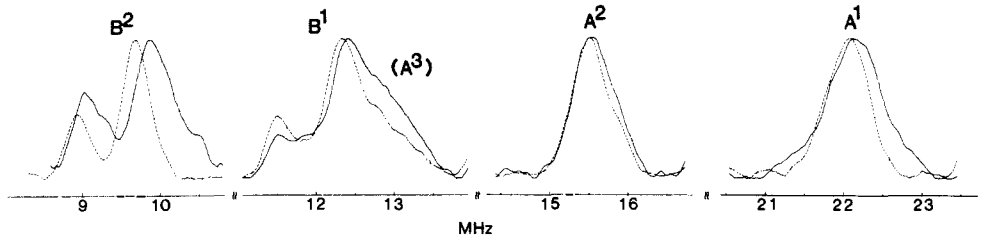

Figure 4. ^{57}Fe ENDOR of wild-type (---) and V$^-$ (—) Kp1 at $g = g_1'$. The peak numbering and assignments to individual sites are as indicated. The ENDOR spectra were taken in segments, as indicated, with intensities normalized. Conditions are as described in Figure 3 except H_0 = 1570 G and each segment represents ca. 5000 scans.

Table III. Proton Hyperfine Coupling Constants (MHz) for the Wild-Type and NifV$^-$ Kp1 Proteins[a]

	Kp1	NifV$^-$ Kp1		Kp1	NifV$^-$ Kp1
1	3.22	3.14	5	0.62	0.60
2	2.18	2.06	6	0.35	0.34
3[b]	1.66	1.62	7	0.16	0.15
4	0.91	0.89			

[a] Errors are ±0.02 MHz. [b] Exchangeable protons, with the V$^-$ resonances representing two types.

at g_1', only a single site, B^2, is measurably affected by the mutation involved in the V$^-$ cofactor.

It should be noted that the hyperfine coupling values are discussed here in a simplified manner and represent the projection of the hyperfine tensor upon the **g**-tensor axis. Thus, it is not determined whether the change in the hyperfine tensor of the B^2 site represents a change in its principal values or its relative orientation with regard to **g**. However, our experience in simulations[11] favor the former.

^{1}H ENDOR Results. Setting the magnetic field to the high-field edge of the EPR spectrum of wild-type Kp1 in H_2O buffer gives the single-crystal-like proton spectrum at g_3 (Figure 5B). The resonances are centered at the proton Larmor frequency and separated by the hyperfine coupling constant, $\nu_\pm = \nu_H + A_H/2$.[11] The spectrum comprises many (at least six) sets of magnetically equivalent protons, with coupling constants in the range of $0.14 \leq A^H \leq 3.3$ MHz (Table III). The consideration of the shape of the peaks, most noticeably the asymmetry of the ν_+ peak and the shoulder on the ν_- peak of the doublet with the largest coupling, indicates that most resonances probably are associated with multiple types of protons with similar coupling constants. This suggestion is supported by the observation that perturbations of the protein by various agents can give rise to a partial loss of intensity of a doublet. In addition, it is clear that the resolved features are riding an unresolved intensity from other protons. Much of this probably reflects a single broad underlying distant-ENDOR peak, but some of the intensity may be associated with protons of the cluster. The observation of resonances from many protons is clearly consonant with the conclusion obtained from analysis of the Mössbauer data,[16] that the paramagnetism of this center arises from spin coupling among a number of component metal atoms; thus there would be many proton-bearing ligands.

The proton ENDOR spectrum for the NifV$^-$ Kp1 protein in H_2O buffer is shown as Figure 5A. This spectrum is similar to that of the wild-type protein, though comparison shows that the former has poorer resolution in the region associated with a hyperfine coupling constant of 1.67 MHz. Computer subtractions (Figure 5C) of the proton pattern of wild-type from NifV$^-$ Kp1 in H_2O buffer shows that the spectrum of the NifV$^-$ Kp1 has an additional proton doublet that is not present for the wild-type protein. (Figure 5D is discussed presently.)

To obtain evidence regarding coordination sites open to solvent, we examined the proton ENDOR of wild-type and mutant samples

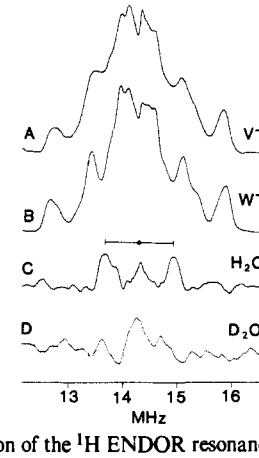

Figure 5. Comparison of the ^{1}H ENDOR resonances of (A) NifV$^-$ (H_2O buffer) and (B) wild-type Kp1 (H_2O buffer) proteins. The digital subtraction (C) = (A) - (B) shows an extra group of strongly coupled protons present in the NifV$^-$ Kp1 protein. The absence of this feature in (D), the digital subtraction of D_2O-exchanged Kp1 WT from D_2O-exchanged NifV$^-$ Kp1, indicates that the extra proton group is exchangeable. Conditions: H_0 = 3362 G; T = 2 K; microwave power, 0.063 mW; microwave frequency, 9.52 GHz; 100-kHz field modulation, 1.25 G; rf power, 20 W; rf scan rate, 0.375 MHz/s; 500 scans.

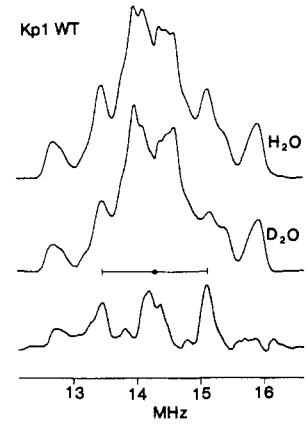

Figure 6. ^{1}H ENDOR spectra at g_3' of WT Kp1 in H_2O and D_2O. The digital subtraction presented below shows a strongly coupled exchangeable proton as well as a diminished distant ENDOR peak in the D_2O sample. Conditions as described in Figure 5.

subjected to D_2O exchange. When the MoFe protein of the wild-type *K. pneumoniae* is subjected to D_2O exchange, there is a reduction in the intensity of the resonance centered at 1.67 MHz (Figure 6). This difference can be assigned to an exchangeable proton, most likely associated with a H_2O or OH^- group coordinated near the metal cluster or with a nearby amide group. The unexchangeable protons could in part represent buried protons that are otherwise exchangeable (e.g., amide), but presumably are mainly structural hydrogens of the amino acid residues that coordinate the metal cluster to the protein. There is also a loss of intensity of the distant ENDOR signal from the solvent.[11]

Upon D_2O exchange NifV$^-$ Kp1 also exhibits a loss of intensity of a proton doublet (Figure 7). However, the peaks in this difference spectrum are broader and correspond to a slightly

(16) (a) Münck, E.; Rhodes, H.; Orme-Johnson, W. H.; Davis, L. C.; Brill, W. J.; Shah, V. K. *Biochim. Biophys. Acta* **1975**, *400*, 32-53. (b) Huynh, B. H.; Henzl, M. T.; Christner, J. A.; Zimmermann, R.; Orme-Johnson, W. H.; Münck, E. *Biochim. Biophys. Acta* **1980**, *623*, 124-138.

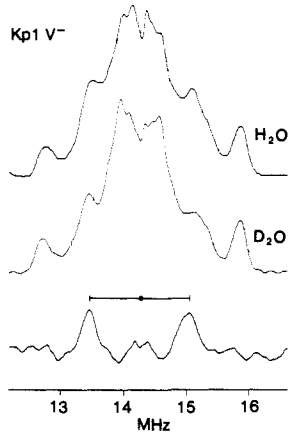

Figure 7. ^1H ENDOR spectra at g_3' of NifV⁻ Kp1 in H_2O and D_2O. Their digital subtraction is presented below. Conditions as described in Figure 5.

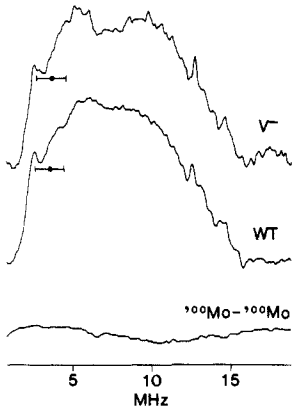

Figure 8. ^{95}Mo ENDOR of Kp1 WT and NifV⁻ Kp1 at $g = g_3'$; each is obtained by subtracting the spectrum of an ^{100}Mo-enriched sample from that of the ^{95}Mo-enriched sample. The hyperfine couplings are described in the text. The bottom trace is the digital subtraction of two separate ^{100}Mo spectra. Conditions: H_0 = 3360 G; T = 2 K; microwave power, 0.2 mW; microwave frequency, 9.52 GHz; 100-kHz field modulation, 4 G; rf power, 20 W; rf scan rate, 2.5 MHz/s; 700 scans.

smaller coupling constant (1.62 MHz) than the exchangeable proton in the wild-type protein, suggesting that they do not merely correspond to the same group of exchangeable proton(s) seen in the wild-type protein. As a final comparison, the difference spectrum obtained by subtracting the traces for D_2O-exchanged wild-type and NifV⁻ protein samples (Figure 5D) is essentially featureless except for a difference in the distant ENDOR signal and does not show the additional proton resonance for the mutant protein in ^1H_2O. We infer that the extra resonance present in the NifV⁻ protein belongs to an exchangeable proton(s) present in the mutant protein but not in the wild-type protein.

^{95}Mo ENDOR Results. When an ENDOR trace, at g_3, of an ^{100}Mo (I = 0) enriched Kp1 sample is computer subtracted from the trace of the ^{95}Mo-enriched protein, a rather broad feature appears in the region of 0–15 MHz (Figure 8). This entire feature is assigned to ^{95}Mo resonances, as numerous subtractions of independent spectra reveal the same feature, whereas subtractions of independent ^{100}Mo-enriched proteins yield a consistent featureless base line.[11] The weak, sharp features in the vicinity of ν_H (~13 MHz) are not significant; they are imperfectly cancelled proton resonances. However, spectra taken at other fields show that the resolved peak at ~2.7 MHz on the low-frequency edge of the ENDOR spectra is significant. As described earlier,[11] this sharp resonance is the ν_- peak of a Larmor doublet associated with the ^{95}Mo, $m_I = \pm^1/_2$, nuclear transition and can be used to obtain the hyperfine coupling in the $S = {}^3/_2$ representation, A_3^{Mo} (Table IV).

The breadth of the ^{95}Mo pattern at g_3' is determined by the satellite ($m_I \neq \pm^1/_2$) transitions and for both the wild-type and

Table IV. ^{95}Mo Hyperfine and Quadrupole Coupling Parameters (MHz) for the Nitrogenase MoFe Protein of *K. pneumoniae*

	A_1	A_3	P_3
NifV⁻ Kpl	5.10 (10)	7.5 (1)	1.6 (1)
Kpl	4.57 (10)	7.4 (1)	1.6 (1)

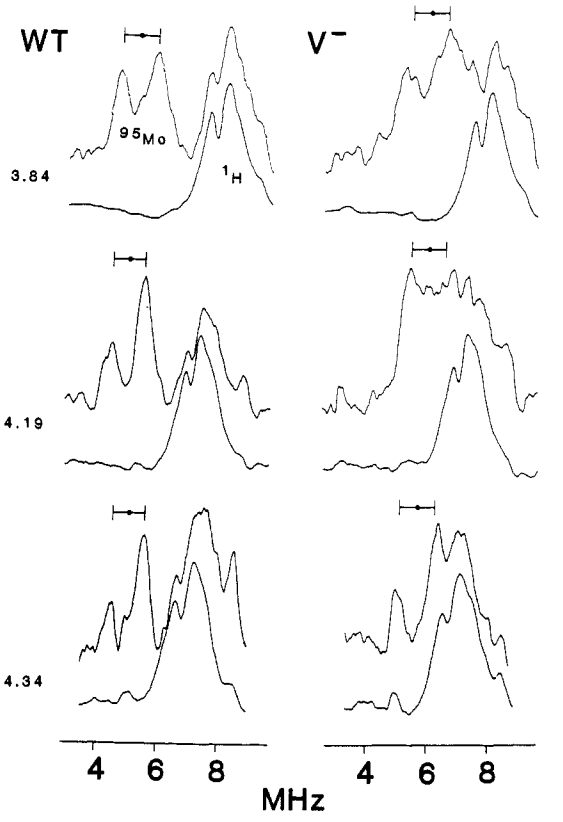

Figure 9. ^{95}Mo ENDOR of Kp1 WT and NifV⁻ Kp1 at g values near g_1. Molybdenum ENDOR spectra of (left) wild-type Kp1 and (right) NifV⁻ Kp1. The g values for each set of paired traces are as listed. The upper spectrum of each pair corresponds to the ^{95}Mo-enriched species and the lower to the analogous ^{100}Mo-enriched protein. Conditions are as described in Figure 8; microwave frequency, 9.52 GHz.

mutant proteins can be given a first-order discussion (eq 3) if we use ν_N^0 = 0.9 MHz, A_3^{Mo} ~7.5 MHz and P_3 ~1.6 MHz. Of course, when the quadrupole coupling is not small compared to the hyperfine interaction, the first-order treatment is adequate for the qualitative discussion presented here but is not quantitatively reliable. The breadth of the ^{95}Mo ENDOR pattern for the NifV⁻ protein is identical with that from the wild-type protein and the quadrupole coupling, $P_3(V^-)$, as well as the hyperfine coupling, $A_3^{Mo}(V^-)$ (Table IV) of the V⁻ and wild-type proteins are indistinguishable.

When the magnetic field is set along the g_1' axis, a complicated spectrum of proton and ^{95}Mo resonances is obtained for a ^{95}Mo-enriched Kp1 sample (Figure 9).[10,11] Comparison of the ENDOR signals at g_1' from the ^{95}Mo-enriched ($I = {}^5/_2$) protein with that of the ^{100}Mo-enriched (I = 0) sample discloses a ^{95}Mo doublet, centered at $A^{Mo}/2$, (~5.0 MHz, Table IV). The doublet becomes clearly resolved as g_{obs} is decreased from g_1' and the increase in observing field, and thus in the proton Larmor frequency, shifts the proton pattern to higher frequency.

This ^{95}Mo doublet is assigned to transitions between the $m_I = \pm^1/_2$ level of the $I = {}^5/_2$ ^{95}Mo nucleus (eq 3), and $A^{Mo}/2$ is listed in Table IV. This assignment is corroborated by the Larmor splitting of the doublet (1.07 MHz), which is as predicted upon inclusion of the pseudo-nuclear effect with Δ = 12.5 cm^{-1} (eq 5).

$$2\nu_{Mo} = 2\nu_{Mo}^0(1 + 0.04A) = 1.04 \text{ MHz at } g_1' \qquad (6)$$

The ^{95}Mo ENDOR spectrum at g_1' thus has the appearance expected for a nucleus of $I = {}^1/_2$, with no hint of the quadrupolar

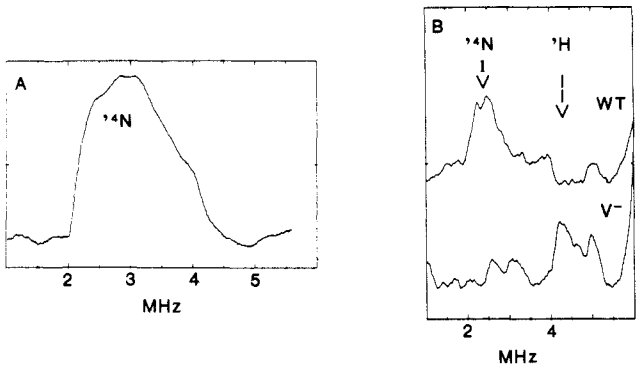

Figure 10. ^{14}N ENDOR of WT and V⁻ Kp1. ^{14}N ENDOR spectra of (A) WT Kp1 at g_3' and (B) WT and V⁻ Kp1 at g_1'. Conditions: H_0 = 3390 G (at g_3'), 1577 G (at g_1'); microwave power, 0.063 mW; microwave frequency, 9.52 GHz; 100-kHz field modulation, 2.5 G; rf power, 20 W; rf scan rate, 5. MHz/s; 1500 scans.

splittings predicted by eq 3, whereas the g_3' pattern is broad, presumably because of such splittings. The characteristics of the ^{95}Mo ENDOR data have been associated[11] with a quadrupole tensor that has P_3(WT) ~1.6 MHz and maximal rhombicity: η ~1 (P_1 ~0, P_2 ~$-P_3$). In such a case, the quadrupole splittings are predicted to vanish when the field lies near g_1' as observed, while at fields above g_2' the quadrupole interactions are thought to cause the satellite transitions to spread over a broad frequency range.[17]

Comparison of the spectra of wild-type and NifV⁻ Kp1 at fields near g_1' unambiguously demonstrates a significant difference in characteristics of molybdenum resonances at g_1' (Figure 9). The ^{95}Mo doublet at NifV⁻ Kp1 is only partly resolved at g_1' because the ^{95}Mo resonances are shifted to higher frequency relative to those of the wild-type protein and partly overlap the proton pattern. However, as the magnetic field is increased, the proton pattern shifts to higher frequency (eq 3), away from the ^{95}Mo resonances. By g' = 3.84 the ^{95}Mo doublet of the NifV⁻ Kp1 sample is clearly distinguishable from the proton pattern and clearly falls at a frequency significantly different from that of the WT protein. From these and other spectra[11] and eq 4, we estimated the following tensor components: WT, A_1^{Mo} = +4.65 (10) MHz; NifV⁻, A_1^{Mo} = +5.15 (10) MHz.[18]

^{14}N ENDOR Results. When the magnetic field is set to g_3' = 2.01, a broad resonance (line width 1.8 MHz) centered at ~2.9 MHz is observed in the wild-type protein (Figure 10A). This feature is present in every sample, with or without isotopic enrichment, and cannot be attributed to ^{57}Fe, ^{95}Mo, or ^{1}H ENDOR resonances. As such, we suggest that this resonance be assigned to ^{14}N ENDOR. At g_1' (Figure 10B), the ^{14}N ENDOR pattern is partly obscured by the proton resonances (ν_H = 6.7 MHz), and due to the poor resolution and low intensity of the peaks when compared to the proton resonances, it is impossible to determine the hyperfine and quadrupole parameters of the site. The ^{14}N ENDOR pattern at g_1' in the NifV⁻ protein, which has less intensity relative to the proton patterns than the wild-type ENDOR data, has two weak features centered at ~2.8 MHz. This difference in intensity is not considered to be significant and could be attributed to either different relaxation properties of the ^{14}N nuclei or to overlapping of the ^{14}N signal with the ^{1}H signal. Although the data from the NifV⁻ protein is not of high quality, the observation of ^{14}N resonances from both the NifV⁻ and the wild-type proteins demonstrates that the coupled nitrogen is present in the mutant protein.

The determination of the primary structure of the MoFe protein of nitrogenase suggests that there are not enough cysteinyl ligands to coordinate all the Fe/S clusters and the FeMo-co clusters in the MoFe protein. Indirect evidence for nitrogen or oxygen donor ligands to molybdenum[9] and less definitely to iron[19] was previously suggested by EXAFS data. More recently electron spin echo (ESE) studies on the MoFe protein and the isolated FeMo-co from *Clostridium pasteurianum* have shown evidence for at least one nitrogen atom associated with the paramagnetic cluster.[20] This ^{14}N resonance, seen in ENDOR and ESE studies, might originate from amide groups from the amino acid residues that coordinate the paramagnetic FeMo-co to the polypeptide backbone, from either the local or remote nitrogen of a covalently coordinated histidine ligand, or even from a nitrogen atom present in the Tris buffer.

Summary

The nifV mutant MoFe protein of *K. pneumoniae* is unlike the wild-type enzyme in that it exhibits poor dinitrogen fixation and inhibition of hydrogen evolution by carbon monoxide. The *nifV*⁻ strain lacks homocitrate, which restores the biosynthesis of wild-type cofactor when added to an in vitro system.[8c] The phenotype of the nifV mutant is transferred to wild-type apoprotein upon addition of mutant cofactor, indicating that the cofactor cluster in the nifV strains is functionally different from that in the wild-type protein. However, the metal ion composition is unchanged in the NifV⁻ protein.[7] Though the EPR line width for NifV⁻ Kp1 is consistently broader, the electronic parameters between the wild-type and mutant cofactors are similar, indicating that the wild-type and NifV⁻ cofactors are not distinguished by a major conformational rearrangement.[7c] This corroborates EXAFS studies that show that the local S and Fe environments of the molybdenum in the two proteins are similar if not identical.[9,10] The ENDOR measurements described here have allowed us to compare at a microscopic level the resting state of the catalytically active center of MoFe proteins isolated from wild-type and NifV⁻ Kp1. ENDOR spectroscopy provides the first physical evidence of a difference between the wild-type and mutant protein.

The characteristics of the molybdenum site differ significantly between wild-type Kp1 and NifV⁻ Kp1. This is evident by the 12% shift in the ^{95}Mo hyperfine coupling constant at g_1'. However, the quadrupole coupling constant, P_3, is roughly the same between the proteins.

The ^{57}Fe ENDOR measurements reveal five magnetically distinct iron sites in both the wild-type and the NifV⁻ cofactors.[11] One iron site, B^2, shows an unambiguous although small shift in its hyperfine coupling constant, indicating that perhaps this site is the closest to the alteration in the mutant cofactor. Because the shifts are slight, it suggests that modification of the cofactor does not directly involve the iron sites.

Evidence for hyperfine coupling to a nitrogenous moiety is presented here. This corroborates ESE data,[20] which show at least one nitrogenous species with a small Fermi contact coupling and large quadrupole coupling. Comparison of the spectra from WT and V⁻ Kp1 indicates that they do not differ by the loss of the nitrogeneous moiety. In contrast, the NifV⁻ Kp1 protein contains exchangeable proton(s) not present in the wild-type Kp1. Although this proton might be from a nearby amide group, most likely it is from a solvent water or hydroxyl group coordinated to the spin center.

This set of observations leads us to suggest that the mutant cofactor cluster is not an isomer of the wild type, but differs by the addition, subtraction, or replacement of non-sulfur metal ligands weakly bound at or near molybdenum (although they do not rule out changes to sulfur ligands distant from molybdenum).

(17) (a) Cohen, M. H.; Reif, F. *Solid State Phys.* **1957**, Vol. 5. (b) Das, T. P.; Hahn, E. *Solid State Phys.* **1958**, *Suppl. 1*. (c) Abragram, A. *Nuclear Magnetism*; Oxford University Press: Oxford, UK, 1960.

(18) (a) EPR line-broadening (ref 18b) confirms that A_3^{Mo} is small, although the quantitation might be affected by isotopic dilution. Note also that ^{17}O line-broadening measurements (ref 18b) can be unreliable for detecting small couplings (see ref 18c). (b) George, G. N.; Bare, R. E.; Jin, H.; Stiefel, E. I.; Prince, R. C. *Biochem. J.* **1989**, *262*, 349–352. (c) Merkle, H.; Kennedy, M. C.; Beinert, H.; Hoffman, B. M. *J. Biol. Chem.* **1986**, *261*, 4840–4846.

(19) Antonio, M. R.; Teo, B.-K.; Orme-Johnson, W. H.; Nelson, M. J.; Groh, S. E.; Lindahl, P. A.; Kauzlarich, S. M.; Averill, B. A. *J. Am. Chem. Soc.* **1982**, *104*, 4703–4705.

(20) (a) Thomann, H.; Morgan, T. V.; Jin, H.; Burgmayer, S. J. N.; Bare, R. E.; Stiefel, E. I. *J. Am. Chem. Soc.* **1987**, *109*, 7913–7914. (b) Note that observation of a nitrogen coupling with small A is not proof of direct Fe ligation, ref 20c. (c) Anderson, R. E. Ph.D. Dissertation, The University of Michigan, 1972.

In *nifV*⁻ strains *homo*citrate may be replaced by the common metabolite citrate during the biosynthesis of the cofactor.[8c] We speculate that the additional exchangeable proton detected in the ^{1}H ENDOR of *nifV*⁻ protein may be on a water molecule present in a cavity that owes its existence to the replacement of *homo*citrate by citrate, either as a template ligand during cofactor biosynthesis or as a component (or component precursor) in the finished cofactor entity.

Acknowledgment. This work was supported by Grants DMB89-07559 (B.M.H.) and DMB85-20687 (W.H.O.-J.) from the National Science Foundation Biophysics Program and by Grant 87-CRCR-1-2430 from the USDA (B.M.H.). The ENDOR spectrometer was purchased with a grant from the NSF Biological Instrumentation Program (PCM-8116106) and received support from the National Institutes of Health (HL-13531, B. M.H.) and the Northwestern University Materials Research Center under the NSF-MRC Program (DMR 8216972).

Registry No. FeMoCO, 72994-52-6; Fe, 7439-89-6; Mo, 7439-98-7.

NMR Studies of the Dinuclear Iron Site in Reduced Uteroferrin and Its Oxoanion Complexes

Robert C. Scarrow, Joseph W. Pyrz, and Lawrence Que, Jr.*

Contribution from the Department of Chemistry, University of Minnesota, 207 Pleasant St. S.E., Minneapolis, Minnesota 55455. *Received December 19, 1988*

Abstract: The chemical shifts and relaxation behavior of paramagnetically shifted proton NMR resonances of reduced uteroferrin (Uf_r) and its XO_4^{n-} complexes (n = 2: X = Mo, W; n = 3: X = P, As) are reported. Integrations with respect to an internal standard show that downfield resonances (δ > 14 ppm vs TMS) arise from 10 protons on ligands to the paramagnetic dinuclear iron center of Uf_r and upfield resonances (δ < −10 ppm vs TMS) arise from at least two protons. Two downfield and one upfield resonance are lost in D_2O. Binding of molybdate, tungstate, or arsenate of Uf_r at pH 4.9 causes minor changes in δ, whereas anaerobic addition of phosphate results in loss of interpretable NMR signals outside of the −3 to 15 ppm range. Uf_rPO_4 at pH 3 exhibits downfield-shifted resonances somewhat larger than those of the other oxoanion complexes at pH 4.9, which suggests weaker antiferromagnetic coupling in Uf_rPO_4. Primarily on the basis of δ and T_1 values, seven of the paramagnetically shifted resonances are assigned to a single tyrosine bound to iron(III) and to a histidine bound to each of the two iron atoms. Probable assignments are given for other paramagnetically shifted peaks.

Uteroferrin is a glycoprotein of molecular weight 40000 isolated from porcine uteri.[1,2] It is abundantly present in the allantoic fluid of pregnant sows and can also be isolated in high yield (up to 0.5 g per pig) from progesterone-treated gilts.[3] Uteroferrin exhibits phosphatase activity with maximal activity at pH 5 and, unlike many phosphatases, it is not inhibited by tartrate. These properties and its color establish uteroferrin as a member of the "purple acid phosphatases", which have been found in many mammalian species (including humans) as well as in yeast and plants.[4] The mammalian enzymes contain a dinuclear iron center per protein molecule,[5,6] while active preparations of various plant enzymes have been reported to have manganese,[7] iron,[8] and dinuclear iron–zinc centers.[9]

Enzymatically active uteroferrin (Uf_r) contains an antiferromagnetically coupled dinuclear iron center in the mixed-valence oxidation state. The Mössbauer spectrum of Uf_r demonstrates the presence of one ferrous and one ferric ion in each protein molecule,[10] and the low-temperature EPR spectrum of Uf_r consists of signals with principal g values of 1.93, 1.74, and 1.59, indicative of an $S = {}^1/_2$ ground state arising from an antiferromagnetically coupled Fe(II)–Fe(III) spin system.[5] Magnetic susceptibility measurements indicate a coupling constant between the high-spin metal centers of $2J = -19.8 \pm 0.5$ cm^{-1} (for $\mathcal{H} = -2J\mathbf{S}_1\cdot\mathbf{S}_2$).[11]

The visible spectrum of Uf_r consists of a broad feature centered at 510 nm, which is assigned to a tyrosinate-to-iron(III) charge-transfer band by resonance Raman spectroscopy.[12] The comparatively large extinction coefficient of uteroferrin (4000 M^{-1} cm^{-1}) and multiple peaks observed in the visible circular dichroism spectra of both oxidation states of uteroferrin led to the suggestion that two tyrosines are bound to the iron, which remains trivalent in both Uf_r and Uf_o.[5]

Uf_r can bind a variety of oxoanions.[13] Molybdate or tungstate are tightly bound inhibitors ($K_i \approx 4$ μM)[14] of uteroferrin and stabilize the mixed-valence oxidation state. Phosphate and arsenate, on the other hand, are more weakly bound inhibitors (K_i's in the millimolar range)[14] and facilitate the air oxidation of Uf_r.[5,13] We have shown that these latter anions form Uf_r–anion complexes[15] prior to their aerobic conversion to the oxidized anion complex over the course of several hours. The oxoanions affect the spectroscopic properties of uteroferrin[13] and are of interest as models of enzyme–substrate and enzyme–product complexes of the catalytic cycle.

We have previously reported NMR studies of Uf_0 and Uf_r. While Uf_r exhibited well-resolved paramagnetically shifted resonances, Uf_o exhibited no resonances outside the diamagnetic region.[16] In the present paper we report NMR spectra for several

(1) Chen, T. T.; Bazer, F. W.; Cetorelli, J. J.; Pollard, W. E.; Roberts, R. M. *J. Biol. Chem.* **1973**, *248*, 8560–8566.
(2) Baumbach, G. A.; Ketcham, C. M.; Richardson, D. E.; Bazer, F. W.; Roberts, R. M. *J. Biol. Chem.* **1986**, *261*, 12869–12878.
(3) Basha, S. M. M.; Bazer, F. W.; Geisert, R. D.; Roberts, R. M. *J. Anim. Sci.* **1980**, *50*, 113–123.
(4) Antanaitis, B. C.; Aisen, P. *Adv. Inorg. Biochem.* **1983**, *5*, 111–136.
(5) Antanaitis, B. C.; Aisen, P.; Lilienthal, H. R. *J. Biol. Chem.* **1983**, *258*, 3166–3172.
(6) Averill, B. A.; Davis, J. C.; Berman, S.; Zirino, T.; Sanders-Loehr, J.; Loehr, T. M.; Sage, J. T.; Debrunner, P. G. *J. Am. Chem. Soc.* **1987**, *109*, 3760–3767.
(7) Kawabe, H.; Sugiura, Y.; Terauchi, M.; Tanaka, H. *Biochim. Biophys. Acta* **1984**, *784*, 81–89.
(8) Hefler, S. K.; Averill, B. A. *Biochem. Biophys. Res. Commun.* **1987**, *146*, 1173–1177.
(9) Beck, J. L.; de Jersey, J.; Zerner, B.; Hendrich, M. P.; Debrunner, P. G. *J. Am. Chem. Soc.* **1988**, *110*, 3317–3318.
(10) Debrunner, P. G.; Hendrich, M. P.; De Jersey, J.; Keough, D. T; Sage, J. T.; Zerner, B. *Biochim. Biophys. Acta* **1983**, *745*, 103–106.
(11) Day, E. P.; David, S. S.; Peterson, J.; Dunham, W. R.; Bonvoisin, J.; Sands, R. H.; Que, L., Jr. *J. Biol. Chem.* **1988**, *263*, 15561–15567.
(12) (a) Gaber, B. P.; Sheridan, J. P.; Bazer, F. W.; Roberts, R. M. *J. Biol. Chem.* **1979**, *254*, 8340–8342. (b) Antanaitis, B. C.; Strekas, T.; Aisen, P. *J. Biol. Chem.* **1982**, *257*, 3766–3770.
(13) Antanaitis, B. C.; Aisen, P. *J. Biol. Chem.* **1985**, *260*, 751–756.
(14) Pyrz, J. W. Ph.D. Dissertation, Cornell University, Ithaca, NY, 1986.
(15) Pyrz, J. W.; Sage, J. T.; Debrunner, P. G.; Que, L., Jr. *J. Biol. Chem.* **1986**, *261*, 11015–11020.

0002-7863/90/1512-657$02.50/0